The study of secondary effects in vibrational and hydrogen bonding properties of 2-and 3-ethynylpyridine and ethynylbenzene by IR spectroscopy

ARTICLE *in* SPECTROCHIMICA ACTA PART A MOLECULAR AND BIOMOLECULAR SPECTROSCOPY · MAY 2014

Impact Factor: 2.35 · DOI: 10.1016/j.saa.2014.04.166 · Source: PubMed

Spectrochimica Acta Part A: Molecular and Biomolecular Spectroscopy 132 (2014) 215–224

Contents lists available at ScienceDirect

Spectrochimica Acta Part A: Molecular and Biomolecular Spectroscopy

journal homepage: www.elsevier.com/locate/saa

The study of secondary effects in vibrational and hydrogen bonding properties of 2- and 3-ethynylpyridine and ethynylbenzene by IR spectroscopy

Danijela Vojta [a], Ivana Matanović [b,1], Goran Kovačević [c], Goran Baranović [a,*]

[a] Division of Organic Chemistry and Biochemistry, Ruđer Bošković Institute, Bijenička c. 54, 10001 Zagreb, Croatia
[b] Theoretical Division, Los Alamos National Laboratory, NM 87545, USA
[c] Division of Materials Physics, Ruđer Bošković Institute, Bijenička c. 54, 10001 Zagreb, Croatia

HIGHLIGHTS

- If in hydrogen bond donor, $\tilde{\nu}$ (C≡C) is lowered by 9 cm^{-1}.
- If in hydrogen bond acceptor, $\tilde{\nu}$ (C≡C) is raised by 3 cm^{-1}.
- The calculated frequency shifts are also in opposite directions and are rationalised by the changes in the electronic charge distribution.

GRAPHICAL ABSTRACT

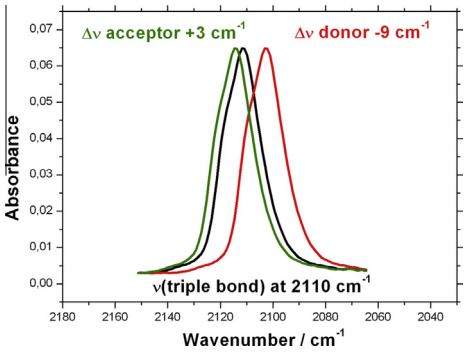

ARTICLE INFO

Article history:
Received 15 January 2014
Received in revised form 18 April 2014
Accepted 23 April 2014
Available online 10 May 2014

Keywords:
Ethynylpyridine
Ethynylbenzene
Hydrogen bonding
IR wavenumber shifts
Anharmonic wavenumbers

ABSTRACT

Weak hydrogen bonds formed by 2- and 3-ethynylpyridine and ethynylbenzene with trimethylphosphate and phenol were characterized by IR spectroscopy and DFT calculations (B3LYP/6-311++G(d, p)). The structure and stability of ethynylpyridines and ethynylbenzene in the gas phase and in the complexes with trimethylphosphate and phenol are discussed in terms of geometry and electronic charge redistribution. Anharmonic effects are taken into account when calculating vibrational wavenumbers of these systems what lead to partial improvement of agreement with experiment. The changes in the electronic charge distribution are behind the frequency shifts of the C≡C stretching in opposite direction depending on the role the ethyne molecule has in a hydrogen bonded complex ($\Delta\tilde{\nu} = +9$ cm^{-1} in trimethylphosphate complexes, $\Delta\tilde{\nu} = -3$ cm^{-1} in phenol complexes). The association constants were determined by keeping the concentrations of proton donors approximately constant and low enough to avoid self-association and the proton acceptors were present in excess. The values obtained for the association constants and enthalpy changes in C_2Cl_4 (for trimethylphosphate complexes $K \approx 0.5$–1.0 mol^{-1} dm^3 and $-\Delta_r H^{\ominus} \approx 6$–$8$ kJ mol^{-1}, for phenol complexes $K \approx 20$–40 mol^{-1} dm^3 $-\Delta_r H^{\ominus} \approx 17$–$22$ kJ mol^{-1}) are in good agreement with literature data.

Introduction

When discussing the multifunctionality of small organic molecules with regard to hydrogen bonding, ethynylbenzene (**eb**)

* Corresponding author. Tel.: +385 1 468 0116; fax: +385 1 468 0195.
E-mail address: goran.baranovic@irb.hr (G. Baranović).
[1] Present address: Department of Chemical & Nuclear Engineering University of New Mexico, Albuquerque, 87131 New Mexico, USA.

http://dx.doi.org/10.1016/j.saa.2014.04.166
1386-1425/

appears as one of the best explored systems. In order to reveal how the presence of a hydrogen bond (HB) accepting or donating group influences the hierarchy between available HB centers (competitive hydrogen bonding), Patwari et al. [1–3] made a comprehensive spectroscopic and computational study regarding the HB affinity of **eb** towards small molecules (water) by employing ≡C—H and =C—H groups of **eb** as HB donating centers and π systems of the C≡C group and phenyl moiety as the HB accepting centers. In addition, they conducted the analogous research on 4-fluoro-ethynylbenzene and 2-fluoro-ethynylbenzene [4] and 4-ethynylbenzonitrile [5].

With this respect, it would be interesting to explore the multifunctionality of ethynylpyridines (**ep**) as well (Fig. 1). Unlike **eb**, **ep** has lone-pair electrons and thus five hydrogen bonding sites. Until now, **ep**s have been studied in the context of crystal engineering. For example, in the monocrystals of 2-ethynylpyridine (**2ep**) and 3-ethynylpyridine (**3ep**) [6] the interplay of weak ≡C—H···N, C—H···N and C—H···π hydrogen bonds, where π designates either C≡C or ring moiety, influences packing of molecules in the solid state. In this way, the engagement of all mentioned HBs results with the shallow zig–zag pattern in **3ep** monocrystal. In contrast, steep zig–zag pattern in **2ep** monocrystal with two symmetry-independent molecules assembled in the perpendicular fashion is governed predominately by the ≡C—H···N HBs. Therefore, **ep**s can be regarded as multifunctional molecules in which variations of HB donating and accepting positions impose a challenge for their application as supramolecular building blocks in both solid state and solution.

To the best of our knowledge, studies of **ep**s that are involved in either weak or medium strong HBs in solution at room temperature and higher do not exist. Therefore, in the present paper, we will characterize **ep**s as both HB donors and HB acceptors in solution by using IR spectroscopy and theoretical approaches. We will compare their acidity to that of ethynylbenzene (**eb**), and their basicity will be compared to that of pyridine (**py**). In order to accomplish these goals, it is essential to expose **ep**s and **eb** to the same HB acceptor (trimethyphosphate (**tmp**) in the present study), and **ep**s and **py** to the same HB donor (phenol (**ph)** in the present study) (Fig. 1).

The acidity of the ≡C—H group has already been extensively reviewed [7]. By using the solute HB acidity and basicity parameters α_2^H and β_2^H for **eb** ($\alpha_2^H = 0.12$, **eb** is thus very weak proton donor and the same is expected for **ep**s) and for **tmp** ($\beta_2^H = 0.76$) [8] it is readily calculated from the equation $\log K(CCl_4) = 7.354\alpha_2^H\beta_2^H - 1.094$ [9] that the association constant for the **eb**···**tmp** complex should be 0.38 mol^{-1} dm^3. Not much different values are to be found for the other two complexes. In comparison with the HB between **ph** and **tmp** for which the measured association constant $K(20\,°C) = 183$ mol^{-1} dm^3 [10] or $K = 173$ mol^{-1} dm^3 when calculated from Abraham's parameters ($\alpha_2^H = 0.596$ for ph), the HBs studied here are thus three orders of magnitude weaker.

In order to explore basicity of **ep**s and **eb**, we have chosen **ph** as HB donor (Fig. 1). HBs between **ph** and pyridine (**py**) and its numerous derivatives, O—H···N, has been characterized by IR spectroscopy [11–14]. The hydrogen bonding basicity of N-atom of pyridine moiety is $\beta_2^H = 0.62$ and for the **ph**···**py** complex it is obtained $K = 43.8$ mol^{-1} dm^3. Banks et al. [15andreferencestherein] report measured values from 41 to 53 mol^{-1} dm^3 at 25 °C.

It has also been known for some time that formation of a HB complex may cause frequency upshifting of the acceptor normal modes [16]. Further studies supported by DFT calculations have shown that significant charge transfer from the acceptor to the donor takes place leading to shortening of some ring bonds and subsequent increase of normal mode frequencies [14,17]. In this paper similar subtle effects of the HB formation as revealed by vibrational analysis of experimental spectra supported by DFT calculations of vibrational harmonic and anharmonic wavenumbers will be discussed. It will be shown that HB formation affects the C≡C stretching vibration in monosubstituted ethynes with the frequency shift being dependent on the role (acceptor or donor) of ethyne molecule in a HB dimer. Frequency shifts of other modes could have not been observed because the concentration of HB complex being always smaller than the analytical concentrations of donor and acceptor was too low. In other words, to study weak HBs ternary mixtures have been prepared (donor and acceptor dissolved in an "inert" solvent) and not the binary mixtures (donor and acceptor fully miscible) as was done in the case of pyridine and related heterocycles and water [14].

Experimental

2-Ethynylpyridine (**2ep**, dark brown liquid at room temperature, b.p. = 85 °C at 12 mmHg, purity 99%), 3-ethynylpyridine (**3ep**, solid at room temperature, m.p. = 39–40 °C, purity 99%), and trimethylphosphate (**tmp**, colorless liquid at room temperature, b.p. = 192–194 °C, purity 99+ %) were purchased from Aldrich. Ethynylbenzene (**eb**, dark yellow liquid at room temperature, b.p. = 142–144 °C, purity 99%), pyridine (**py**, colorless liquid at room temperature, b.p. = 115 °C, purity 99+ %) and tetrachloroethene (C_2Cl_4, colorless liquid at room temperature, b.p. = 122 °C, spectroscopic grade) were purchased from Acros Organics. All the chemicals were used as received. Phenol (**ph**, white crystalline solid at room temperature, m.p. = 40–41 °C, pro analysis), purchased from Kemika, was additionally purified by recrystallization. Densities of the studied liquids were determined by a densitometer DMA 5000-Anton Paar.

All the details about the solution preparation (concentration ranges, the analysis of errors in the association constant

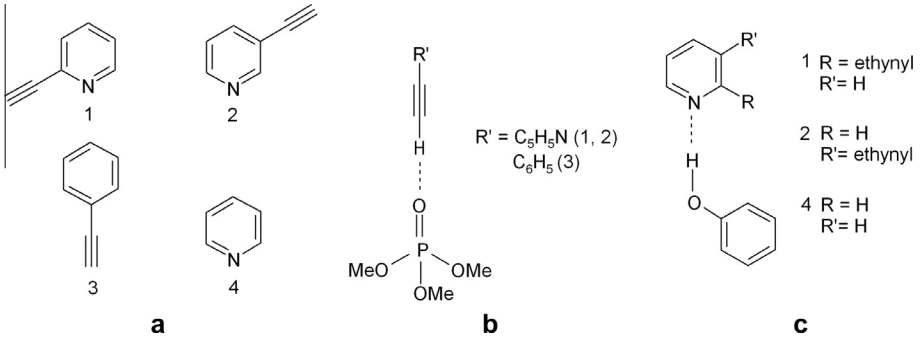

Fig. 1. (a) 1 – 2-ethynylpyridine (**2ep**), 2 – 3-ethynylpyridine (**3ep**), 3 – ethynylbenzene (**eb**), 4 – pyridine (**py**); (b) expected HBs between **ep**s or **eb** and **tmp** and (c) between **ph** and **ep**s or **py**.

determination due to the uncertainties in concentrations, concentration corrections due to temperature, evaluation of association constants from the whole set of experimental data) can be found in Supplementary Information.

IR spectra were measured on an ABB Bomem MB102 spectrometer, equipped with CsI optics, a DTGS detector and a Specac 3000 Series high stability temperature controller with heating jacket. All spectra were measured with nominal resolution of 2 cm^{-1} and 10 scans. The spectral subtraction results that has been extensively used in this work were considered reliable as long as the width of a band was at least 6 cm^{-1}, i.e. three times larger than the nominal resolution of 2 cm^{-1}. IR measurements of solutions at room temperature under atmospheric pressure in air have been performed by using the sealed cells equipped with CaF_2 windows and of nominal pathlengths of 5, 1, 0.5, 0.2 and 0.1 mm. In all the measurements the cell path length was determined by Bertie's procedure using either dichloromethane (CH_2Cl_2) or benzene (C_6H_6) as a secondary standard [18]. The data for each sample were collected three times. Between sequential measurements with the same solution, the cell was emptied, dried with N_2, washed twice with the studied solution; the cell is then refilled and the data were recollected.

Temperature dependent IR spectra of solutions, both binary and ternary, were measured in a CaF_2 sealed cell with d = 984.19 μm and in the temperature range 25–115 °C. The heating rate was 2 °C min^{-1} and the sample was held for 3 min at the given temperature before measuring the spectrum. Temperature difference between the sequential spectra was 10 °C. The spectra of pure solvent were measured in the same temperature interval.

Calculations

Since M0-62X functional is considered as one of the best suited DFT functionals for main-group thermochemistry and non-covalent interactions [19] it was our first choice in geometry optimization and calculations of vibrational properties. However, it has performed rather bad in predicting anharmonic corrections and therefore was replaced with B3LYP functional that gave rather good results in describing the second order (anharmonic) effects in similar systems [20]. What was particularly disappointing in the case of M0-62X was, for example, very low value of 3072 cm^{-1} for the ≡CH stretching in **eb**. This and the $\tilde{\nu}$ (OH) values calculated for complexes with **ph** that were also unreasonably low point to the unsuitability of the M0-62X functional for this type of a problem. Being optimized to reproduce well the energies of HB complexes, the M0-62X functional did not perform well in vibrational frequency calculations when the shape of the potential energy surface around the minimum is probed. The B3LYP exchange–correlation functional has thus been used to optimize the geometries and calculate the frequencies of monomers **ph**, **py**, **2ep**, **3ep** and **eb** and of the complexes with **ph** and **tmp**. Triple-zeta basis set 6-311++G(d, p) with diffuse functions on both, heavy and hydrogen atoms was chosen in order to more accurately describe hydrogen bonding. Only the HBs between ≡C—H moiety of **2ep**, **3ep** and **eb** and O=P moiety of **tmp** and only dimers **ph**···**2ep**, **ph**···**3ep** and **ph**···**py** with the O—H···N HB were considered as these complexes were previously shown to have the higher stability than dimers with HB towards π-electron clouds [21,17]. The initial structures of the complexes were chosen such that the HB structural parameters had reasonable (empirical) values while with the initial dihedral angles all close contacts between the monomers were avoided. Dissociation energies were calculated as a difference between energies of the optimized dimer and energies of the optimized monomers, corrected by basis set superposition error (BSSE). BSSE was corrected with Boys-Bernardi counterpoise correction [22]. Since tetrachloroethene is non-polar solvent with a rather low dielectric constant, ε_r = 2.3, solvent effects on vibrational frequencies and intensities would not be large and were not calculated. All calculations were performed using the Gaussian09 quantum chemical software package [23].

Results and discussion

Calculations of monomer and dimer structures and vibrational spectra

Optimized structures and frequencies of **2ep**, **3ep** and **eb** complexes with **tmp** obtained by using DFT theory (Fig. S1) are expected to faithfully capture the most relevant interactions between monomers. Most relevant structural parameters indicate the principal and secondary interactions identified in the studied complexes. The interactions are confirmed by inspecting the interatomic distances and angles in **ep**s and **eb** induced by the formation of the complex with **tmp** (Table 1). Namely, the distance (≡C—)H···O(=P) = 2.076 ± 0.011 Å is less than the sum of van der Waals radii of (phosphoryl) oxygen and (ethyne) hydrogen which is 1.1 + 1.52 = 2.62 Å. Similarly, for the H···N contact in the complexes with **ph** (Fig. S2) we have 1.872 ± 0.020 Å vs. 2.65 Å. The deviations of the angles ∠(C—H···O) and ∠(O—H···N) from 180° is most pronounced for **2ep** dimer because of the vicinity of ethyne group and the nitrogen atom.

The difference in basicity of the N atom in **2ep** and **3ep** can be estimated from calculated natural charges on these atoms (Table 2). The charge on the N atom in the dimers decreases in the order **ph**···**2ep** < **ph**···**3ep** < **ph**···**py**. Ethynyl group acts as electron-withdrawing group, however this effect is significant only on the N atom in **2ep**. When in HB dimer, the monomers are no longer neutral and the amount of charge transferred is a measure of HB strength. Thus, for example, **3ep** in **3ep**···**tmp** becomes more negative (Δq = −0.014) while in **ph**···**3ep** more positive (Δq = +0.040) (Table 2). According to this criterion it is clear that the HBs with **tmp** are weaker than the HBs with **ph**.

The fact that one of the three methyl groups of **tmp** is directed towards the ethyne moiety implies that it might be involved in a very weak bonding of the C—H···π type (Fig. S1). This secondary interaction is much weaker than the hydrogen bond interaction. However, it seems to be strong enough to contribute to the stabilization of the optimized complex structures. Previous works also found that the proximity of a C—H methyl bond to the N atom lone pair can yields a redistribution of the electronic charge and form a weak hydrogen bond that plays an important role in defining the crystal packing of some molecules [24,25].

Table 1
Selected structural parameters of hydrogen bonded complexes with **ph** and **tmp** calculated at the B3LYP/6-311++G(d, p) level.

Bond lengths (Å) and angles (°)	**2ep**···**tmp**	**3ep**···**tmp**	**eb**···**tmp**
≡C—H	1.072	1.072	1.071
C≡C	1.205	1.206	1.206
C···O	3.128	3.136	3.153
H···O	2.0704	2.0674	2.0900
∠(C—H···O)	168.3	174.1	171.4
∠(C···O—P)	138.2	153.5	147.8
∠(C,C,O,P)	145.0	127.0	60.3
	ph···**2ep**	**ph**···**3ep**	**ph**···**py**
≡C—H	1.063	1.063	1.063
C≡C	1.204	1.205	1.205
O—H	0.982	0.983	0.985
O···N	2.851	2.846	2.832
H···N	1.893	1.870	1.854
∠(O—H···N)	164.5	171.0	171.9
∠(C,O,N,C)	−80.4	−96.9	−95.1

Table 2
Natural atomic charges of the ethyne part and the net natural charge transferred to donor upon HB formation.

	q_N	q_C	Δq	$q_{C\equiv}$	Δq	$q_{\equiv C}$	Δq	q_H	Δq	Charge transferred to donor
eb		−0.137		−0.027		−0.192		0.225		
eb···**tmp**		−0.128	0.009	−0.059	−0.032	−0.185	0.007	0.255	0.030	−0.013
2ep	−0.430	0.115		−0.037		−0.167		0.225		
2ep···**tmp**	−0.438	0.123	0.008	−0.068	−0.031	−0.163	0.004	0.257	0.032	−0.015
ph···**2ep**	−0.487	0.131	0.016	−0.052	−0.015	−0.143	0.024	0.230	0.005	−0.035
3ep	−0.446	−0.172		−0.036		−0.176		0.227		
3ep···**tmp**	−0.450	−0.162	0.010	−0.071	−0.035	−0.163	0.013	0.257	0.030	−0.014
ph···**3ep**	−0.502	−0.163	0.009	−0.044	−0.008	−0.158	0.018	0.229	0.002	−0.040
py	−0.452									
ph···**py**	−0.507									−0.044

The harmonic theory overestimates the frequency of free ≡C—H stretching vibration by 166 cm^{-1} and that of the associated ≡C—H···(O═P) stretching vibration for up to 144 cm^{-1} (Tables 3 and 4). This result is expected as the underlying potential describing the ≡C—H stretching vibration is highly anharmonic. Calculated harmonic frequencies of the fundamental ≡C—H stretching vibration overestimate the experimental values of 3308, 3308 and 3313 cm^{-1} for **2ep**, **3ep**, and **eb**, for up to 190 cm^{-1}. The integrated observed (calculated) intensities of the ε spectra in the interval 3420–3200 cm^{-1} are 32.2 (83.8) km mol^{-1}, 40.3 (97.5) km mol^{-1} and 39.31 (97.2) km mol^{-1} for **2ep**, **3ep** and **eb**, respectively.

When anharmonic corrections calculated using B3LYP/6-311++G(d, p) level of theory are taken into account, ≡C—H stretching frequency downshifts from the harmonic value for about 116 cm^{-1} for monomers and for about 94 cm^{-1} for dimers. The discrepancy between the calculated anharmonic frequencies and experimental values for dimers becomes much smaller and it is 3, 33 and 12 cm^{-1} for **2ep**, **3ep** and **eb**, respectively. This is substantially better than in the harmonic approximation. For the C≡C stretching the anharmonic corrections are much smaller (around 40 cm^{-1}).

The calculated anharmonic wavenumber for the unassociated O—H stretching in **ph** gave only 23 cm^{-1} larger value than experimentally obtained wavenumbers (ν_{obs} = 3610 cm^{-1}) (Table 4). Upon formation of a complex, the calculated wavenumbers corresponding to the same vibration are further lowered by anharmonic correction. The differences with respect to the observed wavenumbers are −11, 2 and −8 cm^{-1} in the case of **ph**···**2ep**, **ph**···**3ep** and **ph**···**py**, respectively meaning that anharmonic wavenumbers are not systematically larger than the observed values. There is thus an additional objection to the widely accepted scaling of harmonic wavenumbers in order to account for the anharmonicity. This is even more dramatic when it has been recognized that anharmonically calculated low-lying wavenumbers could be negative even for the fully optimized geometry pointing thus to insufficient level of approximation applied in their calculations.

IR spectra of binary mixtures at room temperature

We first examine the ethynyl compounds as HB donors, i.e. their acidity. In the region 3360–3260 cm^{-1} of the IR spectra of **2ep** dissolved in C_2Cl_4 three bands occur, at 3330, 3308 and 3290 cm^{-1}, where the central one at 3308 cm^{-1} is by far the most intense (Table S1). Similar situation is observed in the IR spectra of **3ep** dissolved in C_2Cl_4 where, beside the bands at 3330, 3308 and 3287 cm^{-1}, one more weak band at ~3297 cm^{-1} occurs. In contrast to this, two strong bands of comparable intensities, at 3313 and 3302 cm^{-1}, are observed in the **eb** spectra (Table S1, Fig. S3). Since such complex band structure is observed even at the lowest concentrations of **ep**s and **eb** ($c_0 \approx 0.001$ mol dm^{-3}), the possibility

Table 3
Calculated harmonic and anharmonic frequencies (in *italics*) (B3LYP/6-311++G(d, p), in cm^{-1}) for ≡C—H and C≡C stretchings in complexes with **tmp**.

	$\tilde{\nu}$(≡CH)	$\tilde{\nu}$(≡CH···O) Calc.	$\Delta\tilde{\nu}$[a]	$\tilde{\nu}$(≡CH)	$\tilde{\nu}$(≡CH···O) Obs.	$\Delta\tilde{\nu}$	$\tilde{\nu}$(C≡C)	$\tilde{\nu}$(C≡C···) Calc.	$\Delta\tilde{\nu}$	$\tilde{\nu}$(C≡C)	$\tilde{\nu}$(C≡C···) Obs.	$\Delta\tilde{\nu}$
2ep	3476	3352	124	3308	3214	94	2211	2195	16	2120	2111	9
3ep	3475	3356	119	3308	3212	96	2205	2192	13	2116	2107	9
eb	3476	3364	112	3313	3220	93	2202	2189	13	2113	2106	7
2ep	*3349*	*3217*	*132*				*2173*	*2172*	*1*			
3ep	*3349*	*3245*	*104*				*2166*	*2151*	*15*			
eb	*3343*	*3232*	*111*				*2164*	*2154*	*10*			

[a] $\Delta\tilde{\nu} = \tilde{\nu}$(≡C—H) − $\tilde{\nu}$(≡C-H···)*etc*..

Table 4
Calculated harmonic and anharmonic frequencies (in *italics*) (B3LYP/6-311++G(d, p), in cm^{-1}) for O–H and C≡C stretchings in complexes with **ph**.

	$\tilde{\nu}$ (OH)[a]	$\tilde{\nu}$ (OH···N) Calc.	$\Delta\tilde{\nu}$ [b]	$\tilde{\nu}$ (OH)	$\tilde{\nu}$ (OH···N) Obs.	$\Delta\tilde{\nu}$	$\tilde{\nu}$ (C≡C)	$\tilde{\nu}$ (C≡C···) Calc.	$\Delta\tilde{\nu}$	$\tilde{\nu}$(C≡C)	$\tilde{\nu}$ (C≡C···) Obs.	$\Delta\tilde{\nu}$
ph	3836			3610								
2ep		3448	386		3225	385	2211	2215	−4	2120	2123	−3
3ep		3417	419		3185	425	2205	2209	−4	2116	–	–
py		3381	455		3167	443						
ph	*3633*											
2ep		*3214*	*419*				*2173*	*2175*	*−2*			
3ep		*3187*	*446*				*2166*	*2171*	*−5*			
py		*3159*	*474*									

[a] Phenol $\tilde{\nu}$ (OH).
[b] $\Delta\tilde{\nu}$ = $\tilde{\nu}$ (≡C—H) − $\tilde{\nu}$ (≡C—H···) etc.

of self-associations as an explanation of the band shape has been excluded. The possible cause of these and similar phenomena are mechanical or electrical anharmonicities that are not of importance as long as the spectra are only used to calculate association constant K from molar absorption coefficient ε at 3308 cm^{-1} for **ep**s and at 3313 cm^{-1} for **eb**. The molar absorption coefficients ε at the chosen wavenumber (Table S1) were obtained by quadratic fitting of the linear absorption coefficient for **2ep** and linear fitting for other cases.

Before starting the discussion on basicity of ethynyl compounds, it is in order to comment the IR spectra of **ph**. When **ph** is dissolved in C_2Cl_4 the OH stretching band appears at 3610 cm^{-1} (Fig. S4). With an increase in concentration, the band position remains unchanged. As concentration approaches ~0.04 mol dm^{-3}, a very broad band appears centered at approximately 3485 cm^{-1}. Its concentration dependence clearly indicates that the band arises from **ph** self-association. From absorbance values and analytical concentrations of **ph**, ε was determined. By taking only the 14 (12) lowest concentrations up to 0.019 (0.011) mol^{-1} dm^3 and with a linear fit, $\varepsilon = 228 \pm 4$ (236 ± 4) mol^{-1} dm^3 cm^{-1} is obtained. From the quadratic fit of 21 points, $A/d = (0.18 \pm 0.02) + (234.6 \pm 1.1)\cdot c_0 - (509.9 \pm 6.6)\cdot c_0^2$ and $\varepsilon = (d(A/d)/dc_0)(c_0 = 0) = 235 \pm 1$ mol^{-1} dm^3 cm^{-1}. The value reported by Cole, $\varepsilon = 220$ mol^{-1} dm^3 cm^{-1} [26], differs from the present one for ~7% which is not unusual when the thermodynamic quantities are determined by spectroscopic means [11]. From the linearity of the A/d vs. c_0 plot we have concluded that **ph** self-associates to a negligible extent when its initial concentration is below 0.02 mol dm^{-3}. In all the measurements here reported the **ph** concentration was never beyond that limit.

Temperature dependent measurements of binary mixtures

There are changes in the IR spectra of **eb** and **ep**s in the temperature range between 25 and 115 °C, as shown in Fig. S3. The **ep** band at 3308 cm^{-1} and the **eb** band at 3313 cm^{-1} decreases in intensity with temperature. Moreover, the EP band maximum shifts for ~2 cm^{-1} to higher wavenumbers. The **eb** band at 3313 cm^{-1} also shifts to 3315 cm^{-1}, showing thus analogous behavior as the corresponding transitions of **ep**s. Overall behavior is quite expected, i.e. the integrated intensities of the dominant bands decreases while the frequencies increases (0.02–0.03 cm^{-1}/°C) with the increasing temperature. It can be accounted for by the Onsager reaction field theory with temperature dependent solvent refractive index and dielectric constant and the solute molecular cavity [27].

After recording the spectra as a function of temperature, we calculated $\varepsilon(t, 3308\ cm^{-1}) = (252.4 \pm 0.9) - (1.16 \pm 0.02)\cdot(t - 25\ °C)$ for **2ep**, $\varepsilon(t, 3308\ cm^{-1}) = (223.6 \pm 0.4) - (0.929 \pm 0.008)\cdot(t - 25\ °C)$ for **3ep** and for **eb**, $\varepsilon(t, 3313\ cm^{-1}) = (127.5 \pm 0.2) - (0.317 \pm 0.004)\cdot(t - 25\ °C)$. The values of $\frac{1}{\varepsilon_0}\frac{d\varepsilon}{dT} \approx 0.004\ K^{-1}$ are in accord with those found, for example, for amide I band [27]. There is disagreement in the ε values at room temperature determined from concentration measurements and temperature dependent measurements. For example, for **2ep** a value at the room temperature from the fitted line is $\varepsilon(25\ °C, 3308\ cm^{-1}) = 252 \pm 1$ while from the concentration measurements it is obtained in the limit of infinite dilution $\varepsilon(25\ °C, 3308\ cm^{-1}) = 253 \pm 2$ (Table S1). The discrepancy can be considered nonexisting. However, this will not be the case for **ph** (see below).

The temperature increase from 25 °C to 115 °C affects the **ph** O—H stretching band (Fig. S4). The most significant changes concern peak position; it goes from $3609 \pm 1\ cm^{-1}$ (25 °C) to $3614 \pm 1\ cm^{-1}$ (115 °C) at the rate of 0.06 cm^{-1}/°C that is three times faster than for the ≡C—H band. The absorbance decreases as the temperature rises. The temperature dependence of $\varepsilon(t, 3610\ cm^{-1})$ is again linear, $\varepsilon(t, 3610\ cm^{-1}) = (283 \pm 2) - (1.44 \pm 0.04)\cdot(t - 25\ °C)$, in agreement with aliphatic alcohols dissolved in CCl_4 [28]. However, in the present case, $\varepsilon(25\ °C, 3610\ cm^{-1}) = 283\ cm^{-1}$ mol^{-1} dm^3 is much different from the value obtained in the limit of infinite dilution, $\varepsilon(25\ °C) = 236\ cm^{-1}$ mol^{-1} dm^3. When all the available values are taken into account (see Supplementary Information for more details) it is obtained $\varepsilon(t, 3610\ cm^{-1}) = (271 \pm 16) - (1.25 \pm 0.32)\cdot(t - 25\ °C)$ and this was used in association constant calculations of **ph** complexes.

IR spectra of ternary mixtures at room temperature

In ternary systems where HB donor (**ep**s, **eb**) concentration was held approximately constant while the concentration of the HB acceptor (**tmp**) was varied, the most significant spectral changes were observed in the 3360–3155 cm^{-1} spectral range (Fig. S5). The intensities of the bands at 3308 cm^{-1} of **ep**s and 3313 cm^{-1} of **eb** is reduced and a new band at ~3215 cm^{-1} for **2ep**, ~3213 cm^{-1} for **3ep**, and ~3221 cm^{-1} for **eb** emerges. Since the novel band in the IR spectra of **ep**s and **eb** does not occur in IR spectra of **tmp**, **ep**s, and **eb** alone, it is unambiguously due to the HB formation between **tmp** and **ep**s or **eb**. Neither of the bands that appear in 3360–3260 cm^{-1} spectral region shifts with the increase in **tmp** concentration. The corresponding frequency shifts of $\Delta\tilde{\nu} = 93$, 95 and 82 cm^{-1}, respectively, suggest somewhat weaker H bond in the **eb**···**tmp** complex.

The presence of **tmp** also induces certain changes in the C≡C stretching band profile as well (Fig. 2). As discussed in our previous work [20], the C≡C stretching band of **eb** dissolved in C_2Cl_4 is asymmetric on its low-frequency side at room temperature. The origin of the asymmetry is most likely the anharmonic coupling between the C≡C stretching and the sequence of hot bands of probably more than one of the low-frequency vibrational states that are at room temperature significantly populated. As expected, the asymmetric band shape of the C≡C stretching with a maximum at 2120 cm^{-1} is also observed in the IR spectra of **ep**s dissolved in C_2Cl_4 at room temperature. Both the frequencies and the band shape change upon the formation of the complex with **tmp**. The low-frequency side becomes more pronounced and the well-defined bands at 2111 cm^{-1} in **2ep**···**tmp** and 2107 cm^{-1} in **3ep**···**tmp** emerge (Fig. 2). They are stronger than the bands at 2120 cm^{-1} in **2ep** and 2116 cm^{-1} in **3ep**. In the IR spectra of **eb**···**tmp** the low-frequency feature at 2106 cm^{-1} gains intensity with an increase of **tmp** concentration, but it does not exceed the band at 2113 cm^{-1} in non-complexed **eb**. In summary, the C≡C stretching vibrations of **2ep**, **3ep** and **eb** are downshifted by 9, 9 and 7 cm^{-1}, respectively, when in complex with **tmp**. The calculated differences are 16, 13 and 13 cm^{-1}, respectively (Table 3). This should be attributed to the re-distribution of electronic charge when HB complex is formed (Table 2).

The addition of HB acceptor (**ep**s and **py**) to the solutions where HB donor (**ph**) concentration is held approximately constant causes obvious spectral changes (Fig. S6). A very broad feature appears that gains intensity at the cost of the O—H stretching band at 3610 cm^{-1}. In the IR spectra of **ph**···**2ep** and **ph**···**3ep** this feature arises in the spectral range 3250–3100 cm^{-1}. For **ph**···**2ep** its maximum is roughly at $\sim 3225 \pm 15\ cm^{-1}$ and for **ph**···**3ep** at $\sim 3185 \pm 15\ cm^{-1}$. For the range of **ph** concentrations used in this study no convincing evidence for the formation of **ph**···**eb** was observed (the presence of a very weak and broad band at around 3540 cm^{-1} can be taken only as an indication). For the purpose of comparison a HB complex between **ph** and **py** was added to the present study. A much broader and stronger band than in the previous two cases extending from ~3500–2900 cm^{-1} and with a complicated structure on its low-frequency side was observed.

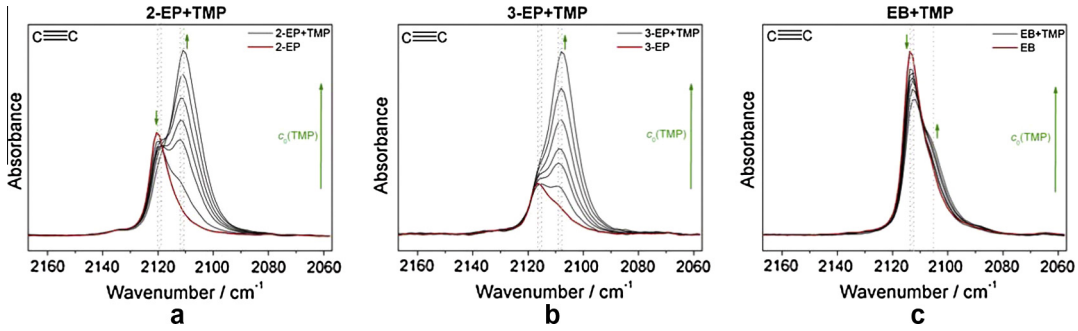

Fig. 2. The C≡C stretching band of **ep**s and **eb** at room temperature in binary (red, C_2Cl_4 subtracted) and ternary mixtures (black, **tmp** in C_2Cl_4 subtracted) with an increase in **tmp** concentration: (a) **2ep**···**tmp**, peaks at 2120 cm^{-1} and 2111 cm^{-1}; (b) **3ep**···**tmp**, peaks at 2116 cm^{-1} and 2107 cm^{-1}; (c) **eb**···**tmp**, peaks at 2113 cm^{-1} and ≈2106 cm^{-1}. (For interpretation of the references to color in this figure legend, the reader is referred to the web version of this article.)

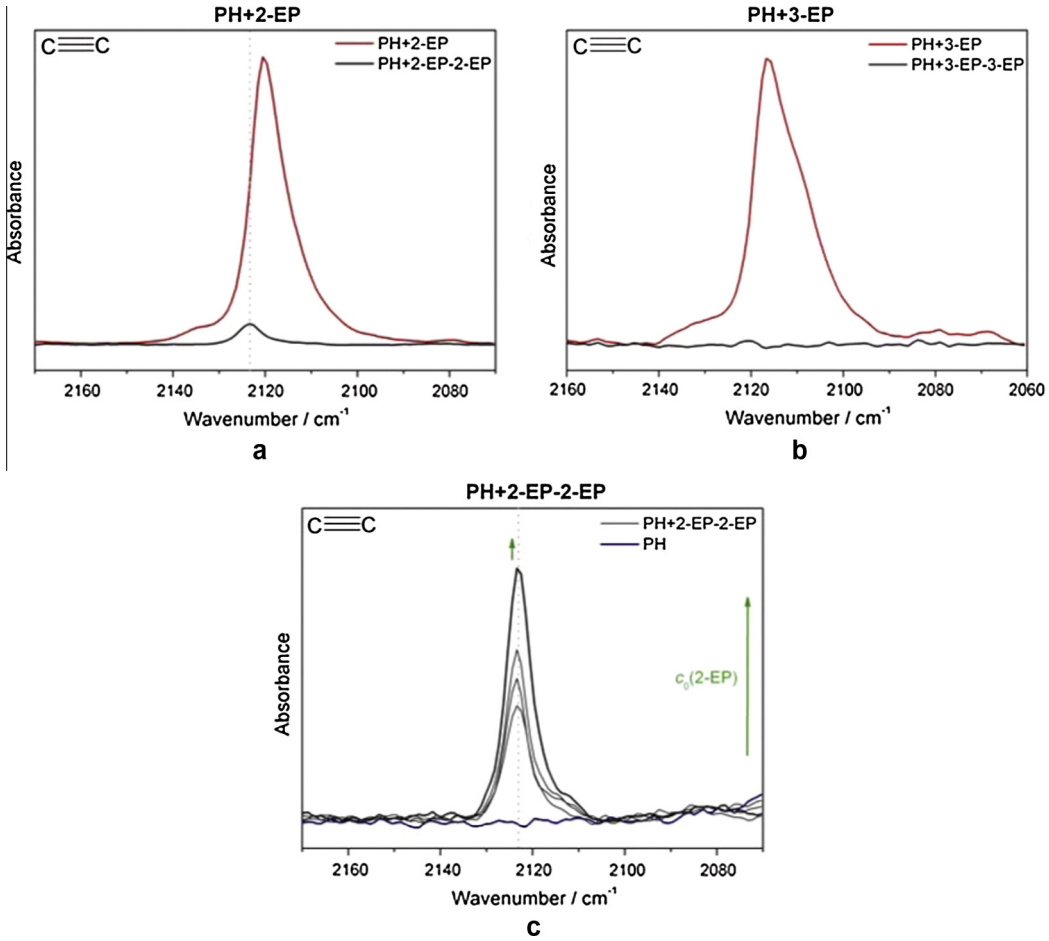

Fig. 3. The C≡C stretching region in the room temperature IR spectra of (a) **ph** + **2ep** mixture (C_2Cl_4 subtracted) and **ph** + **2ep** mixture (**2ep** + C_2Cl_4 subtracted) (c_0(**ph**) = 0.00642 mol dm^{-3}, c_0(**2ep**) = 0.09631 mol dm^{-3}, the stronger band is at 2120 cm^{-1}, the weaker one at 2123 cm^{-1}); (b) **ph** + **3ep** mixture (C_2Cl_4 subtracted) and **ph** + **3ep** mixture (**3ep** + C_2Cl_4 subtracted) (c_0(**ph**) = 0.00493 mol dm^{-3}, c_0(**3ep**) = 0.10037 mol dm^{-3}, peak at 2116 cm^{-1}) and (c) **ph** + **2ep** mixture (**2ep** + C_2Cl_4 subtracted), the peak at 2123 cm^{-1} increases with **2ep** concentration.

The absorption maximum is at around ~3167 ± 10 cm^{-1} [29]. The HB in **ph**···**py** is thus obviously stronger than in the other two complexes.

As seen from Fig. 3, after subtraction of **ep**s spectra from **ph**···**ep**s spectra, the C≡C stretching spectral region looks differently when **ph**···**2ep** and **ph**···**3ep** HB complexes are compared. There is an additional band at 2123 cm^{-1} with the FWHH of 6–7 cm^{-1} due to the **ph**···**2ep** complex. Moreover, this interaction is concentration dependent (Fig. 3c). Therefore, the additional very weak band at 2123 cm^{-1} most likely is due to the HB heterodimers. Its absence in the case of **ph**···**3ep** is explained by the very low intensity of the (C≡C) transition in the complex (Table S2). The wavenumber shifts (Table 4) are negative for both complexes (about −3 cm^{-1}) and this is in agreement with the behavior of pyridine vibrations in HB complexes with water and simple alcohols [16].

Temperature dependent measurements of ternary mixtures

The temperature dependent spectra of **ep**s and **eb** mixtures with **tmp** in C_2Cl_4 revealed changes (Fig. S7) that are the most

prominent in the same spectral region as for the **tmp** concentration dependent spectra (Fig. S5). Since the band originating from the associated ≡C—H oscillator does not disappear even at 115 °C, **ep**s···**tmp** and **eb**···**tmp** complexes live long enough in solution at 115 °C to be captured by IR spectroscopy. The band due to the associated ≡C—H oscillator shifts from 3214 cm^{-1} at 25 °C to 3222 cm^{-1} at 115 °C in the case of **2ep**···**tmp**, from 3212 cm^{-1} to 3220 cm^{-1} for **3ep**···**tmp** and from 3220 cm^{-1} to 3228 cm^{-1} for **eb**···**tmp**. The band intensity decreases with temperature partially as a consequence of decreased number of associated **ep**s and **eb** molecules.

The C≡C stretching band is affected by temperature increase as well (Fig. 4). It shifts for ~1 cm^{-1} to the lower wavenumbers which is negligible. In both binary (Fig. 4a and c) and ternary (Fig. 4d and f) mixtures the band intensity decreases. In the **2ep** spectra, the intensity of the 2111 cm^{-1} band which rises by approximately 50% upon addition of **tmp** at 25 °C, is significantly reduced when the solution is heated up to 115 °C. In the **3ep** spectra the difference in the intensity of the band present only in binary system (Fig. 4b) and the one that appeared with **tmp** added (Fig. 4e) at 25 °C, is even greater than 50%. With an increase in temperature, this difference reduces to approximately 50%. These observations are in agreement with the assumption that C≡C moiety is indirectly involved in the HB formation. At 25 °C in **eb** spectra, when **tmp** is added (Fig. 4f), novel band never prevails the corresponding band in binary mixture spectra (Fig. 4c). By considering the band shapes, the corresponding band in binary mixtures spectra becomes broader on its low-frequency side (red dashed curves). In ternary mixtures spectra (black dashed curves) the band shape from 25 °C to 115 °C remains almost unchanged.

The most significant changes in temperature dependent IR spectra of mixtures of **ph** with **ep**s or **py** appear in the same spectral region as in ternary mixtures recorded at room temperature upon addition of **ep**s or **py** (Fig. S8). The rise of the temperature induces the intensity increase of the O—H stretching band and diminishing of the O—H··· stretching band. The O—H stretching band is shifted to the higher wave numbers by ~6 cm^{-1} which is the same as when only solution of **ph** in C_2Cl_4 is heated. Moreover, the behavior of the O—H band intensity in ternary mixtures above the specified temperatures is analogous to the behavior of the same band in binary mixtures spectra (**ph** in C_2Cl_4).

Since the presence of **ph** induces the appearance of the concentration dependent band of **2ep** at ~2120 cm^{-1}, it is reasonably to expect that it will also be affected by temperature. Therefore, we have analyzed the spectral range 2170–2070 cm^{-1} in the IR spectra of **ph**···**2ep** before and after subtraction of **2ep** in C_2Cl_4 spectra recorded at the same temperature (Fig. 5). The observed decrease in intensity of the high frequency tail of the C≡C stretching profile (Fig. 5a) is analogous to the one exhibited by O-H stretching band of **ph** when involved in HB with **2ep**. This finding makes further support to the hypothesis that C≡C moiety of **2ep** is also affected by the formation of HB.

Determination of the association constants K and $\Delta_r G^{\ominus}$

The calculated association enthalpies (Table 5) are in reasonable agreement with experiment (Table 6), considering that calculations are done within harmonic approximation on isolated molecules in vacuum. The B3LYP calculations thus happened to be close to experimental data. It is informative to compare association energies (ΔE) of complexes since these do not include thermal contributions of molecular motions, but depend solely on bonding between monomers. Among the **tmp** complexes the most loosely bound is **eb**···**tmp**. Among the complexes with **ph** the complex with **py** is most tightly bound. In either case no big difference is predicted between **2ep** and **3ep** complexes.

The values obtained for *K* are presented in Table 6. When the thermodynamic quantities measured in this work are compared with the corresponding ones compiled by Joesten and Schaad [11] it is seen that the values obtained are within the expected intervals, even in the cases of unacceptable large errors. The complexes form spontaneously at lower temperatures. Once *K* is

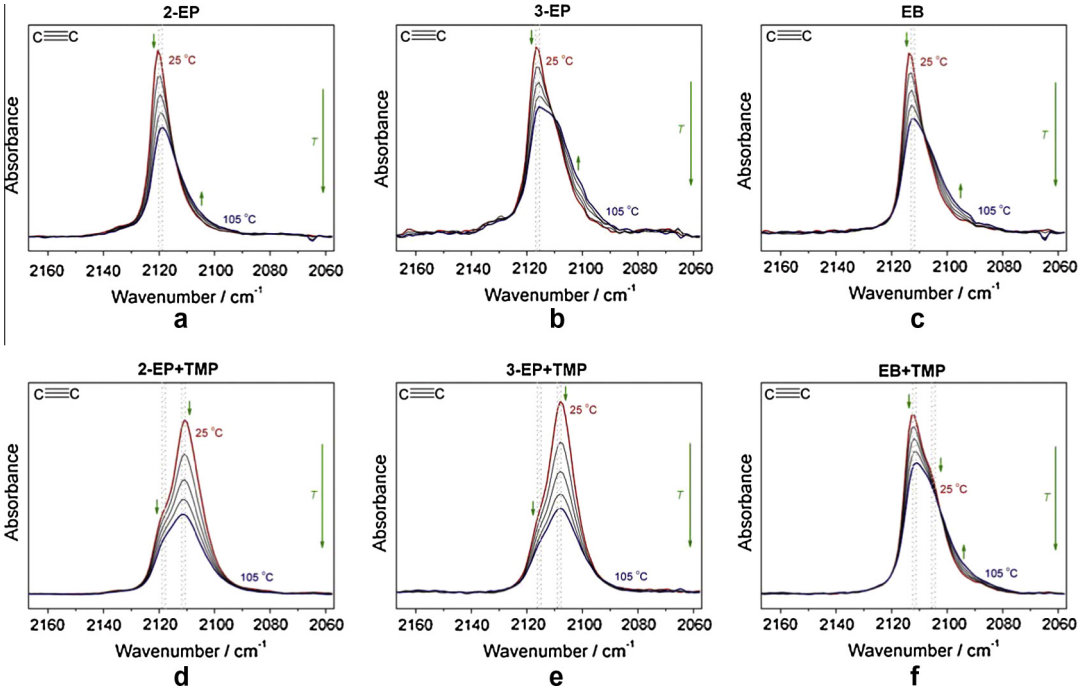

Fig. 4. Temperature study of the C≡C stretching bands (25–115 °C) of **ep**s (a, b) and **eb** (c) in C_2Cl_4 (solvent subtracted) and **ep**s···**tmp** (**d**, **e**) and **eb**···**tmp** (**f**) mixtures in C_2Cl_4 (**tmp** in C_2Cl_4 subtracted): (a) **2ep** (c_0(**2ep**) = 0.05247 mol dm^{-3}); (b) **3ep** (c_0(**3ep**) = 0.05521 mol dm^{-3}); (c) **eb** (c_0(**eb**) = 0.06674 mol dm^{-3}); (**d**) **2ep**···**tmp** (c_0(**2ep**) = 0.05247 mol dm^{-3}, c_0(**tmp**) = 0.91984 mol dm^{-3}); (**e**) **3ep**···**tmp** (c_0(**3ep**) = 0.05521 mol dm^{-3}, c_0(**tmp**) = 0.92479 mol dm^{-3}); (**f**) **eb**···**tmp** (c_0(**eb**) = 0.06674 mol dm^{-3}, c_0(**tmp**) = 0.91798 mol dm^{-3}).

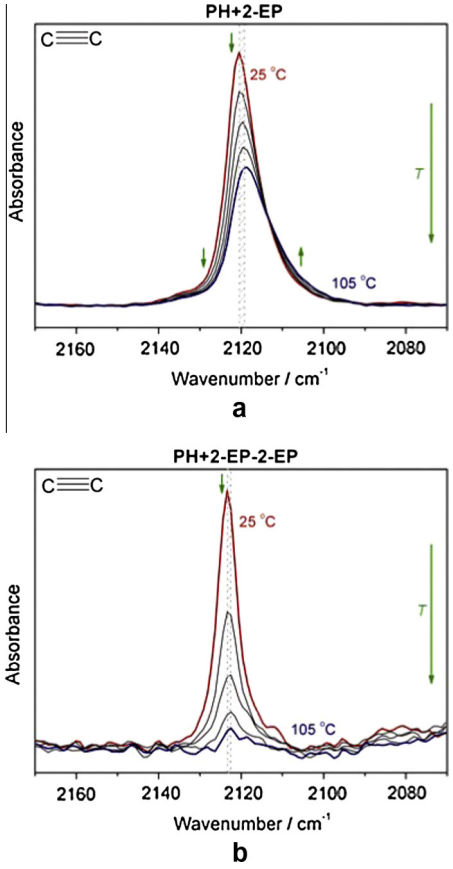

Fig. 5. Temperature study (25–115 °C) of the interval 2200–2000 cm^{-1} of **ph**···**2ep** (c_0(**2ep**) = 0.03762 mol dm^{-3}, c_0(**ph**) = 0.00615 mol dm^{-3}): (a) C_2Cl_4 subtracted, peak shifts from 2120 to 2118 cm^{-1}; (b) **2ep** in C_2Cl_4 subtracted, peak at 2123 cm^{-1} diminishes with temperature.

Table 5
Energies (BSSE corrected values), enthalpies and entropies at 298.15 K for HB complexes of **2ep**, **3ep**, **eb** and **py** with **tmp** and **ph** (B3LYP/6-311++G(d,p)).

Complex	$-\Delta E^a$	$-\Delta G^a$	$-\Delta H^a$	$-\Delta S^b$
2ep···**tmp**	16.7	−21.4	10.4	107
3ep···**tmp**	16.5	−20.8	9.9	103
eb···**tmp**	14.1	−22.4	7. 7	101
ph···**2ep**	31.8	−9.5	25.0	116
ph···**3ep**	31.7	−12.0	24.6	123
ph···**py**	34.2	−4.1	27.2	105

[a] kJ mol^{-1}.
[b] J mol^{-1} K^{-1}.

obtained for the complexes in an inert solvent in stoichiometry 1:1, it is possible to use a general treatment of HB formation in an inert solvent, i.e. the scales of solute hydrogen bonding [9,30,31]. Abraham et al. made all measurements in CCl_4 whereas here they were made in C_2Cl_4. However, the similarity of the molar absorption coefficients in two solvents is expected and it has been found that $\log K(C_2Cl_4) = (0.999 \pm 0.013)\log K(CCl_4) + (0.05 \pm 0.03)$ [32].

The K values at room temperature obtained from the linear regression $-\ln K$ vs. $1/T$ are very small and decreases in the following order: **2ep**···**tmp** ($K = 1.1 \pm 0.3$ mol^{-1} dm^3) > **3ep**···**tmp** ($K = 0.9 \pm 1.1$ mol^{-1} dm^3) > **eb**···**tmp** ($K = 0.55 \pm 0.59$ mol^{-1} dm^3). The values obtained from concentration measurements at room temperature are 0.82 ± 0.06, 0.74 ± 0.05 and 0.46 ± 0.08, respectively. Thus, the complexes of **2ep** and **3ep** with **tmp** are slightly more stable than the complex **eb**···**tmp**. The measured values of Abraham's α_2^H parameters evaluated from $\alpha_2^H = (\log K + 1.1)/4.636$ [9] are $\alpha_2^H = 0.25 \pm 0.03$ for **2ep** and $\alpha_2^H = 0.23 \pm 0.10$ for **3ep**. For **eb**, the value of 0.18 ± 0.10 reasonably matches the reported value of 0.12 [31]. However, from knowing also that $\beta_2^H = 0.76$ for **tmp**, the association constants for **eb**···**tmp**, predicted from $\log K = 7.354 \cdot \alpha_2^H \beta_2^H - 1.094$ [8], is 0.82 mol^{-1} dm^3 agreeing thus reasonably with 0.55 ± 0.59 and 0.46 ± 0.08 determined in this work. As expected, the obtained $\Delta_r H^\ominus$ values indicate that the considered HBs are weak and increase in the following order: −7.9 ± 0.5 kJ mol^{-1} for **2ep**···**tmp**, −6.1 ± 2.0 kJ mol^{-1} for **eb**···**tmp** and −5.3 ± 2.3 kJ mol^{-1} for **3ep**···**tmp**. The values of $\Delta_r S^\ominus$ also increase in the same order: −26 ± 2 J K^{-1} mol^{-1} for **2ep**···**tmp**, −25 ± 6 J K^{-1} mol^{-1} for **eb**···**tmp** and −19 ± 7 J K^{-1} mol^{-1} for **3ep**···**tmp**. The measured difference of −2.6 kJ mol^{-1} in $\Delta_r H^\ominus$ between **2ep**- and **3ep**···**tmp** complexes can be considered quite comparable to the calculated value of only −0.5 kJ mol^{-1}.

The measured K values are 28 ± 33 (21 ± 4) mol^{-1} dm^3 for **ph**···**2ep**, 29 ± 156 (20 ± 3) mol^{-1} dm^3 for **ph**···**3ep** and 47 ± 106 (43 ± 5) mol^{-1} dm^3 for **ph**···**py** (Table 6). The uncertainties are disappointingly large but the differences between the values determined from temperature and concentration measurements are reasonably close. The ε values of unassociated **ph** were determined from relatively broad concentration range, i.e. from c_0(**ph**) ≈ 0.002 mol dm^{-3} to c_0(**ph**) ≈ 0.2 mol dm^{-3}. Preparation of diluted solutions of **ph** (~10^{-3} mol dm^{-3}) is prone to great uncertainty that decreases with concentration. In a prepared set of binary mixtures there are mixtures with concentrations covering two orders of magnitude. In ternary mixtures, however, we were only dealing with low concentrations of **ph** (c_0(**ph**) ≈ 0.005 mol dm^{-3}) and the measurement uncertainties were consequently higher.

The most stable complex is **ph**···**py** followed by **ph**···**2ep** and **ph**···**3ep**. The K value for **ph**···**py** complex at 26 ± 1 °C in C_2Cl_4 reported here is somewhat smaller than majority of those already reported [11]. An effort has been made in this study to avoid

Table 6
Spectroscopic and thermodynamic characteristics of the hydrogen bonds in donor···**tmp** and **ph**···acceptor systems: standard free energies, $\Delta_r G^\ominus$; reaction enthalpies, $\Delta_r H^\ominus$, and entropies, $\Delta_r S^\ominus$, and association constants K at $t = 26 \pm 1$ °C.

HB system	$-\Delta_r G^{\ominus a}$	$-\Delta_r H^{\ominus a}$	$-\Delta_r S^{\ominus b}$	K (25 ± 1 °C)[c]	K (25 ± 1 °C)[d]	$-\Delta_r G^{\ominus e}$
2ep···**tmp**	0.2 ± 0.8	7.9 ± 0.5	26.0 ± 1.8	1.1 ± 0.3	0.82 ± 0.06	−0.5 ± 0.2
3ep···**tmp**	−0.3 ± 3.1	5.3 ± 2.3	18.7 ± 6.9	0.9 ± 1.1	0.74 ± 0.05	−0.8 ± 0.2
eb···**tmp**	−1.5 ± 2.6	6.1 ± 2.0	25.3 ± 5.9	0.55 ± 0.59	0.46 ± 0.08	−1.9 ± 0.4
ph···**2ep**	8.3 ± 2.9	17.5 ± 2.1	30.8 ± 5.8	28 ± 33	21 ± 4	7.4 ± 0.4
ph···**3ep**	8.3 ± 18.5	17.2 ± 7.9	29.9 ± 36.6	29 ± 156	20 ± 3	7.3 ± 0.4
ph···**py**	9.5 ± 5.6	21.7 ± 4.2	40.7 ± 12.5	47 ± 106	43 ± 5	9.1 ± 0.3

[a] kJ mol^{-1}.
[b] J K^{-1} mol^{-1}. The enthalpy and entropy values should be corrected for the RTαP2 = 0.0025 J mol^{-1} term, but this is obviously negligible.
[c] Calculated at $t = 25$ °C from the linear regression $-\ln(K)$ vs. $1/T$.
[d] K obtained only from concentration dependent measurements at room temperature.
[e] Determined from K obtained only from concentration dependent measurements at room temperature.

self-association of **ph** molecules at the investigated concentrations (c_0(**ph**) ~ 0.005 mol dm^{-3}). Smaller K values for **ph**···**ep** complexes than for the **ph**···**py** complex are expected because ethynyl substituted pyridines have lower basicity than pyridine. Abraham's β_2^H parameters for **2ep** and **3ep** from K values for **ph**···**ep** systems are 0.52 ± 0.04 and 0.52 ± 0.03, respectively. The β_2^H parameter for **py** measured here is 0.59 ± 0.02 and it matches excellently the reported value of 0.62 [31]. By using the high dilution method, Arnett et al. measured $\Delta_r H^\ominus$ of the **ph**···**py** complex in CCl_4 and obtained −29.7 kJ mol^{-1} [33]. Gramstad [34] obtained −29.3 kJ mol^{-1} for $\Delta_r H^\ominus$ and 65.3 J K^{-1} mol^{-1} for $\Delta_r S^\ominus$, while Rubin et al. [35] obtained −27.2 kJ mol^{-1} and 58.6 J K^{-1} mol^{-1}, respectively. The measured values of $\Delta_r H^\ominus$ for **ph**···**py** in CCl_4 are from −21 to −32 kJ mol^{-1} [36].

Conclusions

Weak hydrogen bonds formed by **ep**s and **eb** with **tmp** and **ph** were characterized by IR spectroscopy and DFT calculations. The B3LYP exchange–correlation functional and 6-311++G(d, p) basis set were used to study the structure and stability of **ep**s and **eb** in the gas phase and in the complexes with **tmp** and **ph**. No π-type HB complexes were considered because of their irrelevance for the type of experiment that has been here performed. For the first time, anharmonic effects are taken into account when calculating vibrational wavenumbers of these systems. By inspecting the changes in geometrical parameters in optimized structures of **ep**s and **eb** upon complexation with **tmp** and **ph**, we could identify additional weak interactions that contribute to the electronic charge redistribution and consequently to the frequency shifts of the C≡C stretching in opposite direction depending on the role the ethyne molecule has in HB complex. The association constants were determined by keeping the concentrations of proton donors approximately constant and low enough to avoid self-association and the proton acceptors were present in excess. The values obtained for the association constants and enthalpy changes in C_2Cl_4 are in good agreement with literature data.

Acknowledgements

This work was supported by a Grant No. 0982904-2927 from the Ministry of Science, Education and Sport of the Croatian Government. D. Vojta and G. Baranović thank to J. Alerić and T. Parlić-Risović from Croatian Metrology Institute for the measurements of densities of liquids. I. Matanović thanks the LANL LDRD program for a postdoctoral fellowship, U.S. Department of Energy, Energy Efficiency and Renewable Energy for financial support. Los Alamos National Laboratory is operated by Los Alamos National Security, LLC for the National Nuclear Security Administration of the U.S. Department of Energy under contract DE-AC52-06NA25396. This paper has been designated LA-UR-12-26989.

Appendix A. Supplementary material

Supplementary data associated with this article can be found, in the online version, at http://dx.doi.org/10.1016/j.saa.2014.04.166.

References

[1] P. Chandra Singh, B. Bandyopadhyay, G.N. Patwari, Structure of the phenylacetylene–water complex as revealed by infrared-ultraviolet double resonance spectroscopy, J. Phys. Chem. A 112 (2008) 3360–3363.
[2] R. Sedlak, P. Hobza, G.N. Patwari, Hydrogen-bonded complexes of phenylacetylene with water, methanol, ammonia, and methylamine. The origin of methyl group-induced hydrogen bond switching, J. Phys. Chem. A 113 (2009) 6620–6625.
[3] S. Maity, R. Sedlak, P. Hobza, G.N. Patwari, Infrared-optical double resonance spectroscopic measurements and high level *ab initio* calculations on a binary complex between phenylacetylene and borane-trimethylamine. Understanding the role of C—H···π interactions, Phys. Chem. Chem. Phys. 11 (2009) 9738–9743.
[4] S. Maity, G.N. Patwari, Hydrogen bonding to multifunctional molecules: spectroscopic and ab initio investigation of water complexes of fluorophenylacetylenes, J. Phys. Chem. A 113 (2009) 1760–1769.
[5] S. Maity, A. Dey, G.N. Patwari, S. Karthikeyan, K.S. Kim, A combined spectroscopic and ab initio investigation of phenylacetylene–methylamine complex. Observation of σ and π type hydrogen-bonded configurations and fluorescence quenching by weak C–H···N hydrogen bonding, J. Phys. Chem. A 114 (2010) 11347–11352.
[6] V.R. Thalladi, M. Dabros, A. Gehrke, H.-C. Weiss, R. Boese, Crystal engineering with ≡C—H···N and =C—H···N hydrogen bonds, Cryst. Growth Des. 7 (2007) 598–599.
[7] E.A. Gastilovich, D.N. Shigorin, Vibrations of the ethynyl group (C≡C—H), the hydrogen bond, and intramolecular interactions in monosubstituted acetylenes, Russ. Chem. Rev. (Uspekhi Khimii) 42 (1973) 611–624.
[8] M.H. Abraham, P.L. Grellier, D.V. Prior, R.W. Taft, J.J. Morris, P.J. Taylor, C. Laurence, M. Berthelot, R.M. Doherty, M.J. Kamlet, J.-L.M. Abboud, K. Sraidi, G. Guihéneuf, A general treatment of hydrogen bond complexation constants in tetrachloromethane, J. Am. Chem. Soc. 110 (1988) 8534–8536.
[9] M.H. Abraham, P.L. Greillier, D.V. Prior, P.P. Duce, J.J. Morris, P.J. Taylor, Hydrogen bonding. Part 7. A scale of solute hydrogen-bond acidity based on log$K$ values for complexation in tetrachloromethane, J. Chem. Soc. Perkin Trans. 2 (1989) 699–711.
[10] G. Aksnes, T. Gramstad, Intermolecular hydrogen bond association between phenol and organophosphorus compounds, Acta Chem. Scand. 14 (1960) 1485–1494.
[11] D. Joesten, L.J. Schaad, Hydrogen Bonding, first ed., Marcel Dekker Inc., New York, 1974. pp. 155–183.
[12] J.N. Spencer, Hydrogen bond equilibria of phenol-pyridine in cyclohexane, CCl_4 and benzene solvents, J. Phys. Chem. 91 (1987) 1673–1674.
[13] K.V. Berezin, V.V. Nechaev, S.N. Zotov, Hydrogen bond effects on the fundamental vibration frequencies of pyridine, J. Struct. Chem. 45 (2004) 388–394.
[14] A.M. Wright, A.A. Howard, J.C. Howard, G.S. Tschumper, N.I. Hammer, Charge transfer and blue shifting of vibrational frequencies in a hydrogen bond acceptor, J. Phys. Chem. A 117 (2013) 5435–5446.
[15] T. Banks, K.U. Ingold, J. Lusztyk, Measurement of equilibrium constants for complex formation between phenol and hydrogen-bond acceptors by kinetic laser flash photolysis, J. Am. Chem. Soc. 118 (1996) 6790–6791.
[16] H. Takahashi, K. Mamola, E.K. Plyler, Effects of hydrogen bond formation on vibrations of pyridine, pyrazine, pyrimidine, and pyridazine, J. Mol. Spectrosc. 21 (1966) 217–230.
[17] A. Yong Li, H. Bo Ji, L. Juan Cao, Theoretical study on effects of hydrogen bonding on the ring stretching modes of pyridine, J. Chem. Phys. 131 (2009). 164305-1–164305-8.
[18] J.E. Bertie, C.D. Keefe, R.N. Jones, Tables of Intensities for the Calibration of Infrared Spectroscopic Measurement in the Liquid Phase, first ed., Blackwell Science Ltd., Oxford, 1995. p. 13.
[19] Y. Zhao, D.G. Truhlar, The M06 suite of density functionals for main group thermochemistry, thermochemical kinetics, noncovalent interactions, excited states, and transition elements: two new functionals and systematic testing of four M06-class functionals and 12 other functionals, Theor. Chem. Acc. 120 (2008) 215–241.
[20] D. Vojta, G. Baranović, Intramolecular couplings and the secondary structure of the C≡C stretching bands, Vib. Spectrosc. 52 (2010) 178–187.
[21] K. Sundararajan, V. Vidya, K. Sankaran, K.S. Viswanathan, Trimethyl phosphate–acetylene interaction: a matrix-isolation infrared and ab initio study, Spectrochim. Acta A 56 (2000) 1855–1867.
[22] S.F. Boys, F. Bernardi, The calculation of small molecular interactions by the differences of separate total energies. Some procedures with reduced errors, Mol. Phys. 19 (1970) 553–566.
[23] M.J. Frisch, G.W. Trucks, H.B. Schlegel, G.E. Scuseria, M.A. Robb, J.R. Cheeseman, G. Scalmani, V. Barone, B. Mennucci, G.A. Petersson, H. Nakatsuji, M. Caricato, X. Li, H.P. Hratchian, A.F. Izmaylov. J. Bloino, G. Zheng, J.L. Sonnenberg, M. Hada, M. Ehara, K. Toyota, R. Fukuda, J. Hasegawa, M. Ishida, T. Nakajima, Y. Honda, O. Kitao, H. Nakai, T. Vreven, J. A.Montgomery Jr., J.E. Peralta, F. Ogliaro, M. Bearpark, J. J. Heyd, E. Brothers, K.N. Kudin, V.N. Staroverov, R. Kobayashi, J. Normand, K. Raghavachari, A. Rendell, J.C. Burant, S.S. Iyengar, J. Tomasi, M. Cossi, N. Rega, J.M. Millam, M. Klene, J.E. Knox, J.B. Cross, V. Bakken, C. Adamo, J. Jaramillo, R. Gomperts, R.E. Stratmann, O. Yazyev, A.J. Austin, R. Cammi, C. Pomelli, J.W. Ochterski, R.I. Martin, K. Morokuma, V.G. Zakrzewski, G.A. Voth, P. Salvador, J.J. Dannenberg, S. Dapprich, A.D. Daniels, O. Farkas, J.B. Foresman, J.V. Ortiz, J. Cioslowski, D.J. Fox, Gaussian 09, Revision C.01, Gaussian Inc., Wallingford CT, 2010.
[24] M.F. Tufró, R.H. Contreras, J.C. Facelli, Ab initio study of the nitrogen lone-pair proximity effect on a methyl C-H bond in 2-methylpyridine, J. Mol. Struct. THEOCHEM 254 (1992) 271–277.
[25] M.T. Kirchner, R. Boese, A. Gehrke, D. Bläser, Co-crystallization with acetylene. Part III. Molecular complexes with aromatic azacycles, Cryst. Eng. Comm. 6 (2004) 360–366.
[26] A.R.H. Cole, L.H. Little, A.J. Mitchell, Solvent effects in infra-red spectra. O—H and S—H stretching vibrations, Spectrochim. Acta 21 (1965) 1169–1182.

[27] L. Ackels, P. Stawski, K.E. Amunson, J. Kubelka, On the temperature dependence of amide I intensities of peptides in solution, Vib. Spectrosc. 50 (2009) 2–9.
[28] U. Liddel, E. Becker, Infra-red spectroscopic studies of hydrogen bonding in methanol, ethanol, and *t*-butanol, Spectrochim. Acta 10 (1957) 70–84.
[29] J. Brandmüller, K. Seevogel, Infrarotspektroskopische Untersuchung zur Wasserstoffbrücken-bindung bei Pyridin-Alkohol-Gemischen, Spectrochim. Acta 20 (1964) 453–465.
[30] M.H. Abraham, Scales of solute hydrogen-bonding: their construction and application to physicochemical and biochemical processes, Chem. Soc. Rev. 22 (1993) 73–83.
[31] M.H. Abraham, J.A. Platts, Hydrogen bond structural group constant, J. Org. Chem. 66 (2001) 3484–3491.
[32] J. Graton, M. Berthelot, C. Laurence, Hydrogen-bond basicity pK_{HB} scale of secondary amines, J. Chem. Soc. Perkin Trans. 2 (2001) 2130–2135.
[33] E.M. Arnett, L. Joris, E. Mitchell, T.S.S.R. Murty, T.M. Gorrie, P.v.R. Schleyer, Studies of hdrogen-bonded complex fomation. III. Thermodynamics of complexing by infrared spectroscopy and calorimetry, J. Am. Chem. Soc. 92 (1970) 2365–2377.
[34] T. Gramstad, Studies of hydrogen bonding. Part III. Intermolecular hydrogen bond association between nitrogen compounds and methanol, phenol, α-naphtol and pentachlorophenol, Acta Chem. Scand. 16 (1962) 807–819.
[35] J. Rubin, G.S. Panson, Hydrogen bonding. II. Phenol interactions with substituted pyridines, J. Phys. Chem. 69 (1965) 3089–3091.
[36] C. Ouvrard, M. Berthelot, C. Laurence, An enthalpic scale of hydrogen-bond basicity, part 1: halogenoalkanes, J. Phys. Org. Chem. 14 (2001) 804–810.